American Mineralogist, Volume 83, pages 280–287, 1998

Effects of Mg-Fe^{2+} substitution in calcite-structure carbonates: Thermoelastic properties

JIANZHONG ZHANG,[1] ISABELLE MARTINEZ,[2] FRANCOIS GUYOT,[3] AND RICHARD J. REEDER[1]

[1]The Center for High Pressure Research and Department of Geosciences, State University of New York at Stony Brook, Stony Brook, New York 11794, U.S.A.
[2]Institut de Physique du Globe de Paris, Laboratoire Geochimie des Isotopes Stables
Tour 54-64, 1er Etage, 2 Place Jussieu, 75251 Paris Cedex 05, France
[3]Laboratoire de Mineralogie-Crystallographie and IPGP, Tour 16, Case 115, 4 Place Jussieu, 75252 Paris Cedex 05, France

ABSTRACT

In situ X-ray diffraction has been carried out on two siderite samples of different Fe contents simultaneously at high pressure and high temperature in a DIA-type, large-volume apparatus. Unit-cell volumes, measured up to 8.9 GPa and 1073 K have been analyzed using a Birch-Murnaghan equation of state. With K_0' fixed at 4, the derived equation of state parameters are: K_0 = 117(1) GPa, $(\partial K/\partial T)_P$ = −0.031(3) GPa/K, and $\alpha(K^{-1}) = 1.76(35) \times 10^{-5} + 3.46(62) \times 10^{-8}\ T$ for end-member siderite, and K_0 = 112(1) GPa, $(\partial K/\partial T)_P$ = −0.026(2) GPa/K, and $\alpha(K^{-1}) = 2.09(23) \times 10^{-5} + 2.97(39) \times 10^{-8}\ T$ for the Mg-Fe^{2+} solid solution with 60 mol% $FeCO_3$. These results, along with results obtained previously on magnesite using the same experimental technique, indicate that Fe^{2+} substitution for Mg in the $R\bar{3}c$ carbonates results in a linear increase of the room-temperature bulk modulus and its temperature derivative with increasing Fe content. The bulk modulus increases by more than 10% from $MgCO_3$ to $FeCO_3$. This bulk modulus-composition relationship is mainly attributed to differences in the compressibility of the *a* axis with increasing Fe content, even though the *c* axis is more than twice as compressible as the *a* axis for a given composition. The bulk modulus-volume relationship in the Mg-Fe^{2+} carbonates studied is consistent with trends reported in other ferromagnesian minerals, such as oxides, olivines, pyroxenes, silicate spinels, and garnets, in the sense that it deviates from the empirical prediction that the product of K_0 and V_0 is constant. In addition, these observations are consistent with previous suggestions that substitution of alkaline earth elements by the 3-*d* transition metals may yield a different bulk modulus-volume relationship.

INTRODUCTION

The elastic properties of minerals depend on chemical composition, crystal structure, pressure and temperature. It is important to understand the role of each of these variables when characterizing the elasticity of a mineral. Among studies establishing the compositional effect on elastic properties within different mineral groups, minerals with Mg-Fe^{2+} solid solutions have been investigated extensively because of their importance in understanding the Earth's interior. For most ferromagnesian oxides and silicates that have been studied so far, the bulk modulus appears to increase with increasing Fe content although the absolute difference is typically no more than a few percent for complete substitution (see Hazen 1993, and references therein).

The calcite-structure carbonates ($R\bar{3}c$) represent a mineral group that is structurally different from oxides and silicates. The slightly distorted octahedra are exclusively corner-linked through shared O anions of the CO_3 groups, which are rigid, structurally inert components. It is therefore of interest to examine how the elastic properties of ferromagnesian carbonates compare with oxides and silicates. In this regard, several studies have been carried out recently, particularly for end-member $MgCO_3$ (e.g., Markgraf and Reeder 1985; Redfern et al. 1993; Fiquet et al. 1994; Zhang et al. 1997; Ross 1997). However, no measurements have been made simultaneously at high pressure and high temperature for Fe-rich carbonates. Elastic properties of siderite have been studied from ultrasonic measurements at room temperature by Christensen (1972). He also investigated variations in elastic properties with Mg-Fe^{2+} substitution and showed that the shear modulus of siderite is a few percent larger than that of magnesite.

In this work, we have carried out in situ X-ray diffraction studies at pressures and temperatures up to 8.9 GPa and 1073 K on end-member $FeCO_3$ and an Mg-Fe^{2+} solid solution in the same experiment for direct comparison. By combining the present results with those obtained previously on magnesite (Zhang et al. 1997), thermal equation of state parameters and linear compressibilities of crystallographic axes, derived from the pressure-volume-temperature measurements, are examined with respect to

0003–004X/98/0304–0280$05.00

TABLE 1. Chemical compositions of the starting materials

Element	Sid100*	Sid60*
Fe	0.998	0.602
Mg	0.000	0.376
Ca	0.000	0.006
Mn	0.002	0.016

Note: Chemical compositions were obtained by electron microprobe analysis.
* Formula proportions based on 1 cation.

Mg-Fe^{2+} substitution. The effect of such a substitution on calcite-structure carbonates is also compared with that in other mineral groups.

EXPERIMENTAL METHOD

Two natural single-crystal samples of siderite were used as starting materials, and their chemical compositions are listed in Table 1. The end-member siderite (hereafter referred to as Sid100) was obtained from the United States National Museum (no. R11313) and was originally from Tsumeb, Namibia. The siderite sample with 60 mol% $FeCO_3$ (hereafter denoted as Sid60) was obtained from the American Museum of Natural History (no. 40298) and was originally from Morro Velho, Brazil. Both samples were ground in an agate mortar and pestle for the diffraction work. The X-ray diffraction pattern of Sid60 shows no additional phases present in the sample, indicating that Mg, Fe, and minor Mn and Ca are in solid solution.

The experiment was performed using a DIA-type, cubic-anvil apparatus (SAM85) designed for in-situ X-ray diffraction studies at high pressure and high temperature simultaneously (Weidner et al. 1992). An energy-dispersive X-ray method was employed using white radiation from the superconducting wiggler magnet at beamline X17B of the National Synchrotron Light Source, Brookhaven National Laboratory. The incident X-ray beam was collimated to dimensions of 100 × 200 μm, and diffracted X-rays were collected by a solid-state Ge detector at a fixed angle of $2\theta = 7.5°$. The counting time for each diffraction pattern was usually 3 min. Energy discrimination used a multichannel analyzer (MCA) with 2048 channels.

Peak positions were determined by Gaussian peak fitting of the diffracted intensity. The unit-cell parameters were calculated by least-squares fitting using nine to ten diffraction lines based on an hexagonal unit cell. The relative standard deviations in determination of the unit-cell volume are less than 0.1% as shown in Table 2.

The cell assembly used in this study has been described elsewhere (e.g., Weidner et al. 1992; Wang et al. 1994). A mixture of amorphous boron and epoxy resin was used as the pressure-transmitting medium, and amorphous carbon was used as the furnace material. The two siderite samples were studied simultaneously in a single experiment; the powder samples were packed into a boron nitride container (1 mm in diameter and 2 mm long) separated by a layer of NaCl, which also served as an internal pressure standard.

Temperature was measured by a W/Re24%-W/Re6% thermocouple that was positioned at the center of the furnace. Temperature variations over the entire sample length were on the order of 20 K at 1500 K and the radial temperature gradient was less than 5 K at this condition (Weidner et al. 1992). X-ray diffraction patterns were usually obtained for both samples and the NaCl pressure standard in close proximity to the thermocouple junction; errors in temperature measurements were estimated to be less than 10 K. No correction was applied for the effect of pressure on the thermocouple emf.

Pressures were calculated from Decker's equation of state for NaCl (Decker 1971) using lattice parameters determined from X-ray diffraction profiles at each experimental condition. Five NaCl diffraction lines, 111, 200, 220, 222, and 420, were usually used for determination of pressure. The uncertainty in pressure measurements is mainly attributed to statistical variation in the positions of diffraction lines and is less than 0.1 GPa in the pressure range of the study. No evidence of a vertical pressure gradient was indicated at room and high temperatures, as revealed by examination of lattice parameters of NaCl at different locations of the sample container (Weidner et al. 1992).

All the data reported here were obtained by the following procedures. First the samples were compressed at room temperature to about 10 GPa, followed by heating to the maximum temperature of 1073 K. Data were collected at 1073 K and on cooling only, to minimize nonhydrostatic stress built up during the room-temperature compression. The same procedure was repeated several times at lower pressures.

RESULTS AND DISCUSSION

The X-ray data were obtained for two siderite samples at pressures up to 8.9 GPa along isotherms of 300, 473, 673, 873, and 1073 K (Table 2). At ambient conditions, the lattice parameters and unit-cell volume for Sid100 are $a = 4.6907(2)$ Å, $c = 15.3678(14)$ Å, and $V = 292.828(35)$ Å^3, which are in excellent agreement with values from the JCPDS card. For Sid60, the values are $a = 4.6719(5)$ Å, $c = 15.2517(53)$ Å, and $V = 288.314(133)$ Å^3 (Table 2). The unit-cell parameters from the samples recovered after the experiment are essentially identical to those at the beginning (Table 2), indicating no changes in bulk composition or system calibration over the entire experimental P-T range. We note that the oxidation state of Fe in the siderite samples was unknown because the oxygen fugacity (f_{O_2}) was not controlled in the present experiment. The proportion of Fe^{3+} in the siderite samples, however, is believed to be minimal because of the requirement for charge balance. In addition, from a previous study on metallic Fe using the same technique (J. Zhang and F. Guyot, unpublished data), no wüstite was detected at similar pressure and temperature conditions. Thus it can be inferred that the

TABLE 2. Unit-cell parameters at high pressure and temperature

Pressure (GPa)	Sid100			Sid60		
	a (Å)	*c* (Å)	*V* (Å³)	*a* (Å)	*c* (Å)	*V* (Å³)
			300 K			
0.00*	4.6907(2)	15.3678(14)	292.828(35)	4.6719(5)	15.2517(53)	288.314(133)
0.00†	4.6912(6)	15.3644(42)	292.827(81)	4.6701(5)	15.2571(50)	288.168(88)
0.00‡	4.6935(2)	15.3860(80)	293.530			
1.33	4.6814(6)	15.2780(35)	289.966(79)	4.6582(8)	15.1668(44)	285.013(99)
1.63	4.6774(13)	15.2733(69)	289.379(143)	4.6554(9)	15.1518(50)	284.386(112)
2.73	4.6691(4)	15.1758(23)	286.514(53)	4.6432(14)	15.0833(76)	281.623(171)
4.66	4.6523(4)	15.0441(24)	281.990(54)	4.6289(5)	14.9479(25)	277.379(57)
6.58	4.6411(9)	14.9211(60)	278.340(120)	4.6139(8)	14.8319(51)	273.437(99)
7.41	4.6326(9)	14.8843(55)	276.630(124)	4.6050(6)	14.8012(34)	271.825(75)
			473 K			
2.99	4.6713(3)	15.1935(17)	287.120(35)	4.6467(8)	15.0972(51)	282.304(104)
4.92	4.6545(5)	15.0576(29)	282.514(58)	4.6306(5)	14.9704(30)	277.992(59)
6.84	4.6428(8)	14.9329(50)	278.763(99)	4.6160(9)	14.8485(58)	273.998(113)
7.68	4.6346(5)	14.8869(34)	276.918(67)	4.6074(8)	14.8040(52)	272.156(101)
			673 K			
3.34	4.6735(2)	15.2163(12)	287.818(25)	4.6467(8)	15.1234(55)	283.153(109)
5.27	4.6580(5)	15.0811(30)	283.379(60)	4.6359(10)	14.9871(64)	278.940(127)
7.16	4.6452(10)	14.9555(67)	279.479(133)	4.6185(6)	14.8681(40)	274.654(79)
8.04	4.6365(6)	14.8960(36)	277.320(70)	4.6084(8)	14.8256(54)	272.678(106)
			873 K			
3.69	4.6744(7)	15.2679(29)	288.909(71)	4.6543(4)	15.1616(37)	284.430(67)
5.62	4.6614(5)	15.1074(33)	284.279(65)	4.6384(6)	15.0209(35)	279.876(72)
7.53	4.6482(7)	14.9790(45)	280.274(89)	4.6209(5)	14.8998(30)	275.526(60)
8.43	4.6382(4)	14.9193(28)	277.958(54)	4.6118(6)	14.8404(35)	273.353(68)
			1073 K			
4.12	4.6791(21)	15.3082(131)	290.248(290)	4.6589(4)	15.1826(23)	285.392(46)
6.01	4.6649(5)	15.1400(31)	285.321(62)	4.6421(4)	15.0577(27)	281.009(53)
7.91	4.6512(7)	15.0128(45)	281.268(89)	4.6250(3)	14.9343(18)	276.661(35)
8.87	4.6384(3)	14.9489(17)	278.535(34)	4.6131(4)	14.8692(20)	274.036(41)

Notes: The values in parentheses are standard deviations. The measured temperatures for each isotherm are within ±2 K of the indicated values.
* Cell parameters obtained at the beginning of the experiment.
† Recovered after the high pressure and temperature experiment.
‡ From the JCPDs card (No. 29-696).

oxygen fugacity in the experimental charge was below the iron-wüstite buffer.

Unit-cell parameters

The relative compressibilities, a/a_0 and c/c_0, and the volume compressibility, V/V_0, at room temperature are shown as a function of pressure in Figure 1. In the experimental pressure range, compressibility along the *c* axis is more than twice as large as that along the *a* axis. Such anisotropic compression is typical of other rhombohedral carbonates (e.g., Redfern et al. 1993; Fiquet et al. 1994; Martinez et al. 1996; Zhang et al. 1997; Ross 1997). It is also evident in Figure 1 that Sid60 is more compressible than Sid100, even though V/V_0 values for the two siderite samples are within 2 estimated standard deviations (esd) of one another at some pressures.

At room temperature, the linear compressibilities along the *a* axis (β_a) and *c* axis (β_c) and the volume compressibility (β_V) for Sid100 are $1.66(4) \times 10^{-3}$ GPa^{-1}, $4.35(6) \times 10^{-3}$ GPa^{-1}, and $7.58(8) \times 10^{-3}$ GPa^{-1}, respectively. For Sid60, these values are $1.87(5) \times 10^{-3}$ GPa^{-1}, $4.10(5) \times 10^{-3}$ GPa^{-1} and $7.89(10) \times 10^{-3}$ GPa^{-1}. The expected relation $\beta_V \approx 2\beta_a + \beta_c$ is observed for the two siderite samples within errors of fitting the experimental data. At higher temperatures, similar patterns of linear compressibilities are found. For example at 1073 K, β_a and β_c are $1.75(6) \times 10^{-3}$ GPa^{-1} and $4.81(11) \times 10^{-3}$ GPa^{-1} for Sid100, and $2.02(3) \times 10^{-3}$ GPa^{-1} and $4.26(4) \times 10^{-3}$ GPa^{-1} for Sid60.

Room-temperature bulk modulus

The Birch-Murnaghan equation of state (EOS) has been often used to fit isothermal compression data for compounds of different structures, even though this equation was developed, strictly speaking, for cubic materials. For materials that are highly anisotropic, such as siderite in this study, it is obvious that structural response to compression along crystallographic axes can be understood better in terms of linear compressibilities. However, to facilitate direct comparison with published EOS parameters, the Birch-Murnaghan EOS was adopted here for fitting the room-temperature volume data shown in Figure 1 and listed in Table 2 for Sid100 and Sid60. It is given by

$$P = 3/2K_0[(V_0/V)^{7/3} - (V_0/V)^{5/3}]\{1 + 3/4(K_0' - 4) \cdot[(V_0/V)^{2/3} - 1]\} \quad (1)$$

where V_0 is the molar volume at ambient conditions, and K_0 and K_0' are the isothermal bulk modulus and its pres-

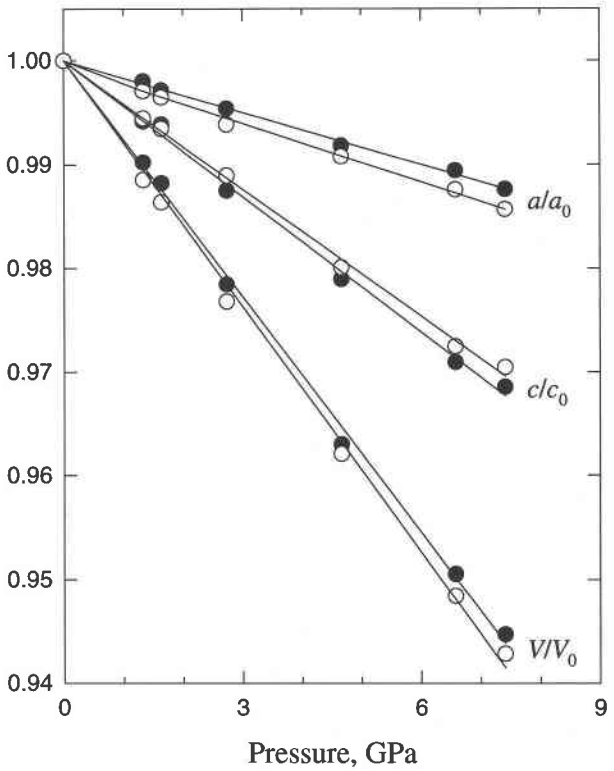

FIGURE 1. Variations of a/a_0, c/c_0, and V/V_0 as a function of pressure at room temperature. Closed symbols = Sid100; open symbols = Sid60. Straight lines represent results of linear least-squares fitting for β_a, β_c, and β_V. Errors in the unit-cell parameters are smaller than the symbol sizes (see Table 2), which is also true in Figure 2.

sure derivative at 300 K. Due to the limited pressure range of the current experiment, K_0' could not be defined well from the finite strain method and was therefore assumed to be 4 and independent of temperature in the subsequent data analysis. The V_0 values for the two siderite samples were also fixed for reasons discussed below. For Sid100, we obtained K_0 = 117(1) GPa and for Sid60, K_0 = 112(1) GPa. Our room-temperature bulk modulus for Sid100 is close to the adiabatic value of Christensen (1972) obtained from ultrasonic measurements (see Table 3).

It is well known that the K_0 values are dependent on the K_0' values. To gain some sense of the variation of K_0 for different K_0' values, we calculated additional fits using K_0' values of three and five. The results, listed in Table 3, show that even though K_0 is sensitive to the choice of K_0', the difference among K_0 values essentially remains constant. Further experiments would, of course, be needed to constrain the K_0' value more precisely.

Another source of uncertainty comes from the fact that slightly different K_0 values are obtained if V_0 is treated as a fitting parameter. For Sid100, for example, we obtain V_0 = 293.14(16) Å^3 and K_0 = 114(2) GPa for K_0' = 4. For this approach, however, the fitted V_0 value, even within error, is different from the measured V_0 (see Table 2), which is obviously the best-constrained data point among the measured P-V data for Sid100.

TABLE 3. Comparison of thermoelastic parameters for different fitting constraints

	K_0' = 3	K_0' = 4	K_0' = 5
	Sid100		
K_0, GPa	120(1)	117(1)	114(1)
$(\partial K_T/\partial T)_P$, GPa/K	−0.026(3)	−0.031(3)	−0.036(4)
α_0 (× 10^5)	1.66(33)	1.76(35)	1.81 (39)
α_1 (× 10^8)	3.19(56)	3.46(62)	3.79 (70)
	Sid60		
K_0, GPa	115(1)	112(1)	109(1)
$(\partial K_T/\partial T)_P$, GPa/K	−0.020(2)	−0.026(2)	−0.031(3)
α_0 (× 10^5)	1.98(22)	2.09(23)	2.17(27)
α_1 (× 10^8)	2.71(36)	2.97(39)	3.29(47)

Thermal equation of state

The volume data in the experimental P-T space are shown in Figure 2. These data were analyzed using the high-temperature Birch-Murnaghan (HTBM) EOS (Saxena and Zhang 1990). In the HTBM EOS, Equation 1 is modified in the following two aspects: (1) the temperature dependence of the bulk modulus is included, given by:

$$K_T = K_0 + (\partial K_T/\partial T)_P(T - 300) \quad (2)$$

and (2) V_0/V is replaced by V_T/V, where V_T is the molar volume at high temperature and ambient pressure and is calculated from

$$V_T = V_0\exp[\int\alpha(T)\mathrm{d}T]. \quad (3)$$

In our analysis, $\alpha(T)$ is expressed as

$$\alpha(T) = \alpha_0 + \alpha_1 T. \quad (4)$$

The tradeoff between K_0' and other thermoelastic parameters has also been explored (Table 3), and the results of the analysis using K_0' = 4 are summarized in Table 4, along with results of previous studies along the join $FeCO_3$-$MgCO_3$. It can be seen in Table 3 that the $(\partial K_T/\partial T)_P$ values are also sensitive to the values of K_0'. Hereafter the discussion is based on analyses using K_0' = 4.

The pressure derivative of thermal expansion is an important parameter for defining the thermal equation of state of solids and is directly related to the change of bulk modulus with temperature by the thermodynamic identity:

$$(\partial\alpha/\partial P)_T = K_T^{-2}(\partial K_T/\partial T)_P. \quad (5)$$

Using thermoelastic parameters obtained from the HTBM EOS (Table 4), cell volumes at a given (constant) pressure were calculated at steps of 200 K in the temperature range 300–1073 K; average thermal expansivities were calculated for the two siderite samples and plotted in Figure 3 as a function of pressure. These calculations reveal that the pressure dependence of thermal expansion for Sid100 is slightly larger than that for Sid60. Linear regression of the data in Figure 3 yields $(\partial\alpha/\partial P)_T = -2.22 \times 10^{-6}$

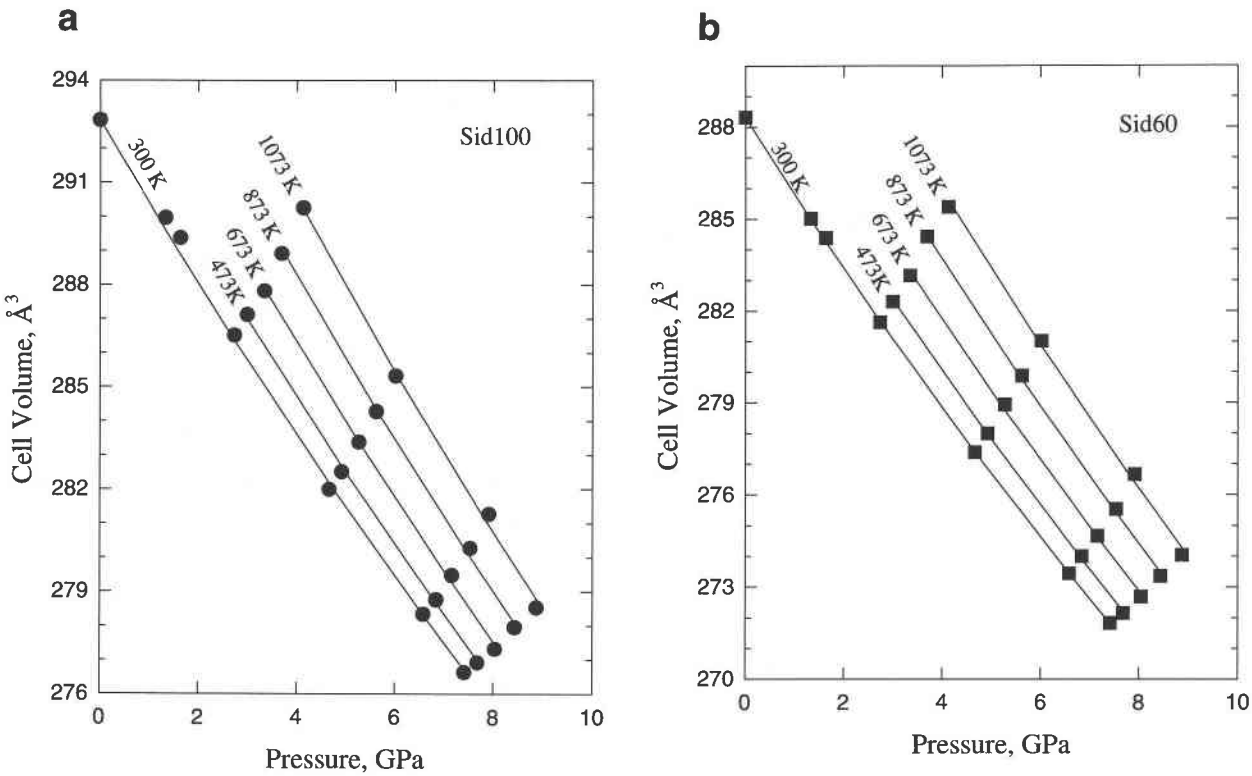

FIGURE 2. *P-V-T* diagrams showing the entire data set used to calculate the HTBM EOS for Sid100 (**a**) and Sid60 (**b**) (see text for discussion). The solid curves between 300 and 1073 K represent polynominal fits to the data points, at intervals of 200 K above 300 K.

$K{\cdot}GPa^{-1}$ for Sid100 and -1.95×10^{-6} $K{\cdot}GPa^{-1}$ for Sid60. From Equation 5, values of $(\partial K_T/\partial T)_P$ are calculated to be −0.030 and −0.025 GPa/K, respectively, for Sid100 and Sid60. As expected, these values are consistent with those obtained directly from the HTBM EOS (Table 3).

Effects of Fe^{2+}-Mg substitution

Room-temperature bulk modulus. The room-temperature bulk moduli of the two siderite samples are compared with that of magnesite (Zhang et al. 1997) in Figure 4a and 4b as functions of composition and cell volume at ambient conditions. Fe^{2+} substitution for Mg results in a nearly linear increase of the bulk modulus with increasing Fe content (Figure 4a). The bulk modulus increases by more than 10% from $MgCO_3$ to $FeCO_3$. This relative increase is about twice as large as that reported for adiabatic bulk moduli in the work of Christensen (1972) from ultrasonic measurements. Because it is unlikely that such large differences should exist between adiabatic and isothermal bulk moduli at 300 K, one possible explanation for this discrepancy is the difference in composition between the samples investigated; in the study of Christensen (1972), magnesite contained 7 mol% $CaCO_3$ and siderite contained up to 13 mol% other carbonate components.

The effect of Mg-Fe^{2+} substitution in calcite-structure carbonates is similar in magnitude to that in silicate spinels, which show a 13% increase in the room-temperature bulk modulus from Mg_2SiO_4 to Fe_2SiO_4 (Hazen 1993). The same trend has also been observed in other ferromagnesian silicates and oxides, although the difference in bulk modulus is typically less than a few percent for com-

TABLE 4. Equation of state parameters of ferromagnesian carbonates

Source	K_0 (GPa)	$(\partial K_T/\partial T)_P$ (GPa/K)	$\alpha(K^{-1}) = \alpha_0 + \alpha_1 T$ α_0 ($\times 10^5$)	α_1 ($\times 10^8$)	$(\partial\alpha/\partial P)_T$ ($\times 10^6$K/GPa)
		$FeCO_3$			
This study	117 (1)	−0.031(3)	1.76(35)	3.46(62)	−2.22
Christensen (1972)	116	—	—	—	—
		$(Fe_{0.6}Mg_{0.38}Mn_{0.02})CO_3$			
This study	112(1)	−0.026(2)	2.09(23)	2.97(39)	−1.95
		$MgCO_3$*			
Zhang et al. (1997)	103(1)	−0.022(2)	3.15(17)	2.32(28)	−1.76

Note: Except for $(\partial\alpha/\partial P)_T$, all the parameters in this table are the results of fitting from the HTBM EOS (see text) at $K_0' = 4$. K_0 of Christensen (1972) is adiabatic whereas all others are isothermal.

* The EOS parameters obtained from other studies (e.g., Christensen 1972; Redfern et al. 1993; Fiquet et al. 1994; Ross 1997) are not used for comparison because systematic errors may exist in some or all of the experiments on magnesite.

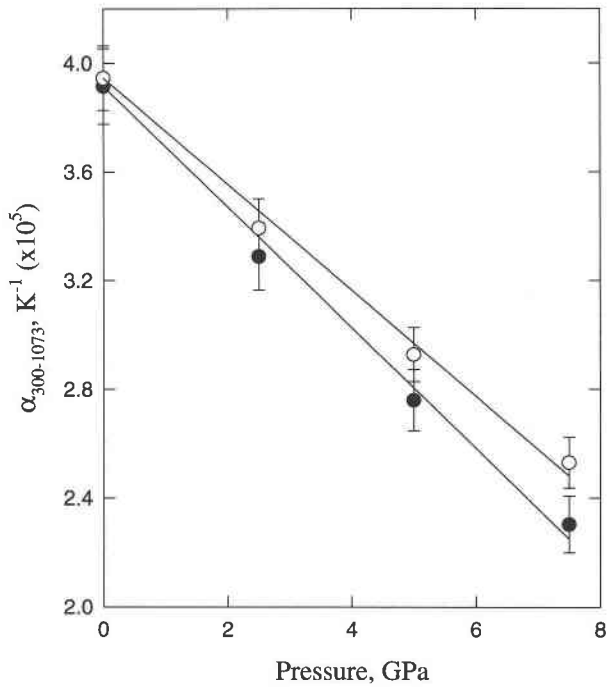

FIGURE 3. Thermal expansion coefficient plotted as a function of pressure. The term $\alpha_{300-1073}$ denotes average thermal expansivity in the temperature range 300–1073 K. Closed symbols = Sid100; open symbols = Sid60. Uncertainties represent errors of least-squares fitting of the volume-temperature data obtained using the method described in the text. Straight lines represent results of fitting for $(\partial\alpha/\partial P)_T$.

plete substitution (e.g., Sumino 1980; Hazen 1993, and references therein). In the dolomite-structure carbonates, where two metal atoms are ordered between alternating layers with the CO_3 groups, the polyhedral bulk moduli of MgO_6 in dolomite and $(Mg_{0.3}Fe_{0.7})O_6$ in ankerite are 98 and 101 GPa, respectively, even though the bulk modulus of dolomite is slightly larger than that of ankerite (Ross and Reeder 1992).

It is obvious that the trend shown in Figure 4b does not follow the commonly accepted bulk modulus-volume systematics: For many oxides and silicates of the same crystal structure, the product of the room-temperature bulk modulus and the molar volume has been observed to be a constant and independent of the mean atomic mass (Anderson and Anderson 1970; Chung 1972). However, it appears to be a common feature of ferromagnesian minerals, such as olivines (Sumino 1977, 1979), pyroxenes (Zhang et al. 1997), silicate spinels (Hazen 1993), and garnets (Babuska et al. 1978; Zhang et al. 1996), that the bulk moduli deviate from the "K_0V_0 = constant" relationship. For oxides, direct comparison is complicated by the fact that wüstite is non-stoichiometric and generally contains some Fe^{3+}.

The bulk compressibility of many compounds is controlled primarily by the compressibilities of their constituent polyhedra, which are largely determined by the mean cation-oxygen bond length in the polyhedra (Hazen and Prewitt 1977; Hazen and Finger 1982). In the calcite-structure carbonates, the CO_3 groups are essentially incompressible, rigid units; in magnesite, for example, the C-O distance ($d_{C\text{-}O}$) does not vary by more than 2 esd between room pressure [$d_{C\text{-}O}$ = 1.288(2) Å] and 7 GPa [$d_{C\text{-}O}$ = 1.283(3) Å], and the polyhedral bulk modulus of MgO_6 was found to be nearly identical to the bulk modulus of $MgCO_3$ (Ross 1997). These observations are con-

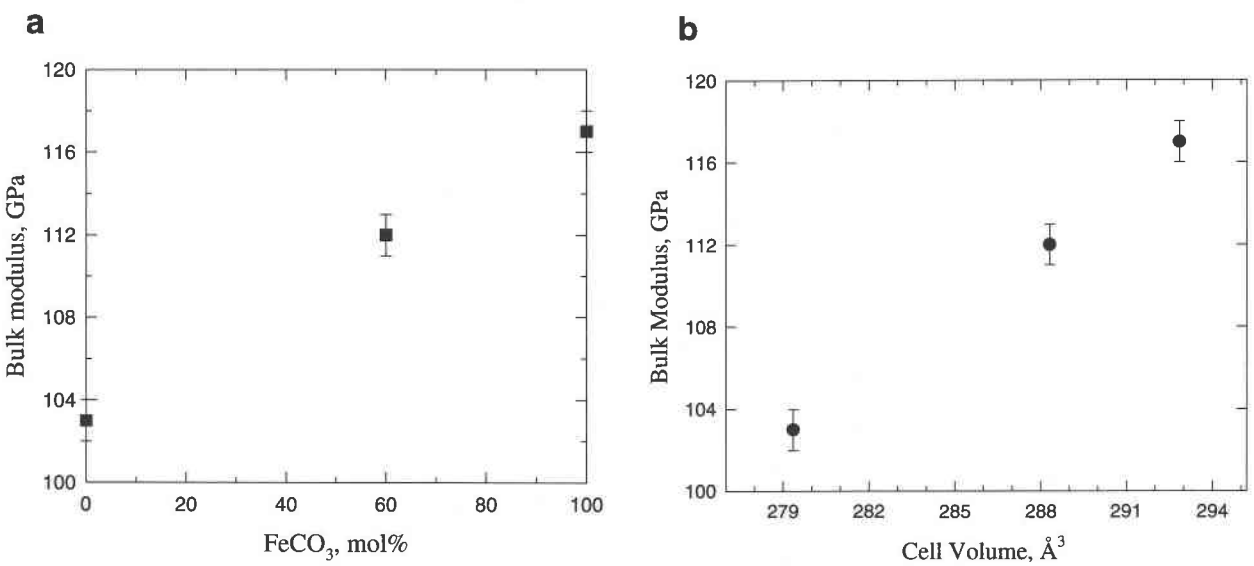

FIGURE 4. Room-temperature bulk modulus as functions of composition (**a**) and cell volume (**b**). Error bars are from the least-squares fit using the HTBM EOS. For magnesite, the bulk modulus is from Zhang et al. (1997).

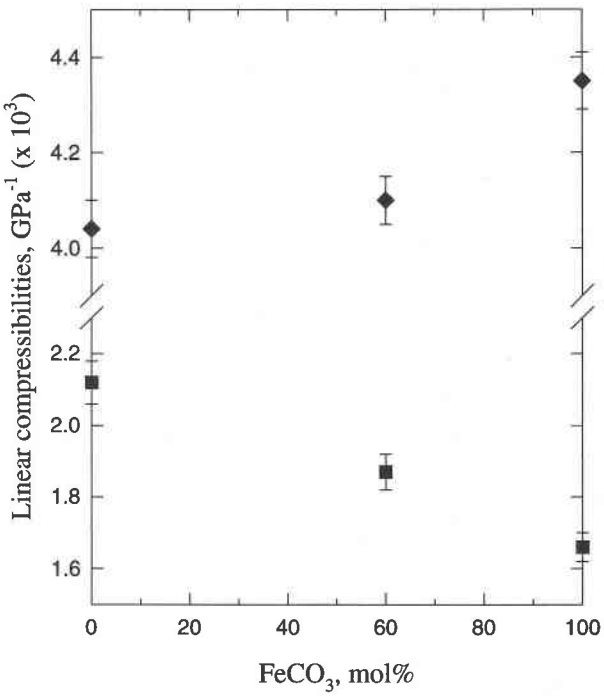

FIGURE 5. Compositional effects on linear compressibilities of ferromagnesian carbonates. Squares = a axis; diamonds = c axis. The data for magnesite are from Zhang et al. (1997). Calculations show that the relative changes of compressibilities are about 28 and 8%, respectively, along the a and c axes for complete Mg-Fe^{2+} substitution.

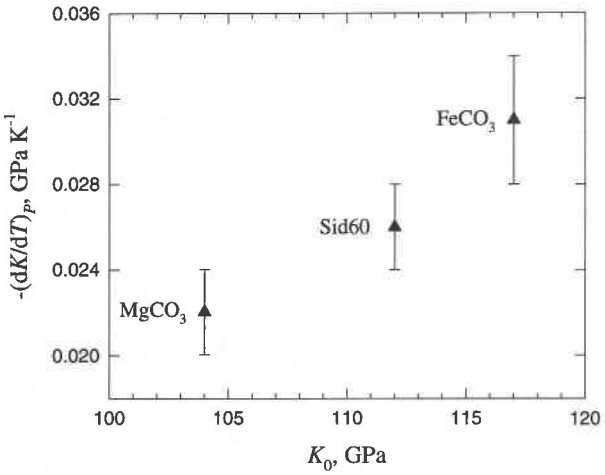

FIGURE 6. Relationship between the room-temperature bulk modulus and its temperature derivative. For $MgCO_3$ (magnesite), the value of $(\partial K_T/\partial T)_P$ is from Zhang et al. (1997).

sistent with previously suggested compression mechanisms. However, the M^{2+}-O distances in magnesite and siderite at ambient conditions are 2.1018(4) and 2.1445(5) Å, respectively (Reeder 1983). The fact that siderite has a larger M^{2+}-O distance than magnesite but is less compressible is inconsistent with the general relation suggested by Hazen and Prewitt (1977) and Hazen and Finger (1982). It is also important to note here that our observations on the $FeCO_3$-$MgCO_3$ join differ from those reported by Martens et al. (1982), in which a linear correlation between the bulk compressibility and M-O bond length was found for carbonates of both the calcite and aragonite structure types. The conclusions of Martens et al. (1982), however, should be viewed with caution because some of the compressibility data they used were taken from other studies; systematic errors in the measurements of compressibilities may exist in some or all of the experiments referenced. For example, the bulk modulus of siderite used in their systematics differs from that of Christensen (1972) and that of this study.

Linear compressibilities at room temperature. It was noted earlier (Fig. 1) that over the entire pressure range studied the a axis of Sid100 is less compressible than the a axis of Sid60. This result is consistent with a previous study on magnesite (Zhang et al. 1997), as shown in Figure 5. Inspection of Figure 5 demonstrates that the compressibility of the a axis decreases almost linearly with increasing Fe content whereas that of the c axis behaves in an opposite manner.

Complete substitution of Fe^{2+} for Mg yields a 28% decrease in the compressibility along the a axis. In contrast, the compressibility of the c axis increases by only 8%. As a result, the change in compressibility of the a axis relative to the c axis is greater by more than a factor of three. Considering that the a axis is expected to contribute approximately twice as much as the c axis to the volume compressibility (i.e., $\beta_V \approx 2\beta_a + \beta_c$), these results indicate that the observed bulk modulus-composition relationship shown in Figure 4a is primarily attributed to the decreasing compressibility of the a axis with increasing Fe content.

Temperature derivative of the bulk modulus. The effects of Mg-Fe^{2+} substitution on $(\partial K_T/\partial T)_P$ are shown in Figure 6 including the previously obtained results on magnesite (Zhang et al. 1997). The trend in Figure 6 indicates that the absolute value of $(\partial K_T/\partial T)_P$ increases with increasing Fe content in the $MgCO_3$- $FeCO_3$ binary system. In addition, a linear correlation between $(\partial K_T/\partial T)_P$ and the room-temperature bulk modulus appears to be robust. We note that the $(\partial K_T/\partial T)_P$-$K_0$ relationships have not been studied systematically for isostructural minerals or compounds of different compositions and deserve future investigation. Because $(\partial K_T/\partial T)_P$ is related directly to $(\partial\alpha/\partial P)_T$ according to Equation 5, it is not surprising that a similar compositional effect on $(\partial\alpha/\partial P)_T$ is also observed, as shown in Table 4.

CONCLUDING REMARKS

It is generally believed that variations in elastic properties are controlled primarily by gross features of the crystal structure. The present observations in ferromagnesian carbonates are, however, consistent with suggestions that elastic properties are particularly sensitive to the replacement of Mg by 3-d transition elements (e.g.,

Weidner et al. 1982). In addition, the observed compositional effect on the room-temperature bulk modulus in this study has been seen in other ferromagnesian minerals such as oxides, olivines, pyroxene, silicate spinels, and garnets.

At least two explanations have been proposed for the observed bulk modulus-volume relationship in ferromagnesian compounds. Hazen (1993) suggested that the relative incompressibility of Fe^{2+}-rich silicate spinels may be partially attributed to the *d* electron repulsion across the shared edges of (Mg,Fe^{2+}) octahedra. Hazen (1993) also noted that the shortest Fe^{2+}-Fe^{2+} distance in Fe_2SiO_4 silicate spinel is 2.9 Å, whereas in fayalite the distance is 3.2 Å. This difference may explain why fayalite is only a few percent less compressible than forsterite (see Table 1 in Hazen 1993). In siderite, the shortest Fe^{2+}-Fe^{2+} distance is 3.729 Å, which is even greater than that in fayalite. However, the Fe^{2+}-C^{4+} distance is considerably shorter at 2.996 Å. Thus it is possible that Fe^{2+}-C^{4+} repulsive interactions may be responsible for the relative incompressibility of Fe^{2+}-rich carbonates, but presently they are not understood.

A second possible explanation relates to the effect of the crystal field of the 3-*d* transition elements on the bulk modulus. This effect was investigated by Ohnishi and Mizutani (1978) for MgO-type oxides. They proposed that the deviation of the bulk modulus in rock-salt oxides from the "K_0V_0 = constant" prediction can be explained by considering the crystal field stabilization energy (CFSE). On the other hand, Sumino (1979) pointed out that the deviation of the bulk modulus of olivine (i.e., Mg_2SiO_4) as transition metal cations for Mg was too large to be accounted for by the CFSE. To examine the effects of the CFSE on the bulk modulus of Fe-rich carbonates, a systematic study of the compressibilities of the calcite-structure carbonates with other 3-*d* transition elements is needed.

Acknowledgments

We thank I. Jackson and D.J. Weidner for their very helpful comments. Reviews by N.L. Ross, A. Shen, and anonymous referee were very helpful. The Center for High Pressure Research (CHiPR) is jointly supported by the National Science Foundation under the grant EAR 89-17563 and the State University of New York at Stony Brook. The in situ X-ray experiment was performed at the X-17b1 beam line of the National Synchrotron Light Source (NSLS) at Brookhaven National Laboratory. This is MPI publication No. 208.

References cited

Anderson, D.L. and Anderson, O.L. (1970) The bulk modulus-volume relationship for oxides. Journal of Geophysical Research, 75, 3494–3500.

Christensen, N.I. (1972) Elastic properties of polycrystalline magnesium, iron, and manganese carbonates to 10 kilobars. Journal of Geophysical Research, 77, 369–372.

Chung, D.H. (1972) Birch's law: Why is it so good? Science, 177, 261–263.

Decker, D.L. (1971) High-pressure equation of state for NaCl, KCl and CsCl. Journal of Applied Physics, 42, 3239–3244.

Fiquet, G., Guyot, F., and Itie, J.P. (1994) High-pressure X-ray diffraction study of carbonates: $MgCO_3$, $CaMg(CO_3)_2$, and $CaCO_3$. American Mineralogist, 79, 15–23.

Hazen, R.M. (1993) Comparative compressibilities of silicate spinels: Anomalous behavior of $(Mg,Fe)_2SiO_4$. Science, 159, 206–209.

Hazen, R.M. and Finger, L. (1982) Comparative crystal chemistry: Temperature, pressure, composition and the variation of crystal structure, 228 p. Wiley, New York.

Hazen, R.M. and Prewitt, C.T. (1977) Effects of temperature and pressure on inetratomic distances in oxygen-based minerals. American Mineralogist, 62, 309–315.

Markgraf, S.A. and Reeder, R.J. (1985) High-temperature structure refinements of calcite and magnesite. American Mineralogist, 70, 590–600.

Martens, R., Rosenhauer, M., and Gehlen, K.V. (1982) Compressibilities of carbonates. In W. Schreyer, Ed., High-pressure researches in geoscience, p. 215–222. Schweizerbart'sche Verlagsbunchhandlung, Stuttgart.

Martinez, I., Zhang, J., and Reeder, R.J. (1996) In situ X-ray diffraction of aragonite and dolomite at high pressure and high temperature: Evidence for dolomite breakdown to aragonite and magnesite. American Mineralogist, 81, 611– 624.

Ohnishi, S. and Mizutani, H. (1978) Crystal field effect on the bulk modulus of transition metal oxides. Journal of Geophysical Research, 83, 1852–1856.

Redfern, S.A.T., Wood, B.J., and Henderson, C.M.B. (1993) Static compressibility of magnesite to 20 GPa: Implications for $MgCO_3$ in the lower mantle. Geophysical Research Letters, 20, 2099–2102.

Reeder, R.J. (1983) Crystal chemistry of the rhombohedral carbonates. In Mineralogical Society of America Reviews in Mineralogy, 11, 1–48.

Ross, N.L. (1997) The equation of state and high-pressure behavior of magnesite. American Mineralogist, 82, 682–688.

Ross, N.L. and Reeder, R.J. (1992) High-pressure structural study of dolomite and ankerite. American Mineralogist, 77, 412–421.

Saxena, S.K. and Zhang, J. (1990) Thermochemical and pressure-volume-temperature systematics of data on solids, examples: tungsten and MgO. Physics and Chemistry of Minerals, 17, 45–51.

Sumino, Y. (1977) Temperature variation of elastic constants of single crystal forsterite between −190 °C and 400 °C. Journal of Physics of the Earth, 25, 377–392.

Sumino, Y. (1979) The elastic constants of Mn_2SiO_4, Fe_2SiO_4 and Co_2SiO_4 and the elastic properties of olivine group minerals at high temperature. Journal of Physics of the Earth, 27, 209–238.

Sumino, Y. (1980) The elastic constants of single crystal $Fe_{1-x}O$, MnO and CoO, and the elasticity of stoichiometric magnesiowustite. Journal of Physics of the Earth, 28, 475–495.

Wang, Y., Weidner, D.J., Liebermann, R.C., and Zhao, Y. (1994) Thermal equation of state of (Mg, Fe)SiO3 perovskite and constraints on composition of the lower mantle. Physics of Earth and Planetary Interior, 83, 13–40.

Weidner, D.J., Bass, J.D., and Vaughan, M.T. (1982) The effect of crystal structure and composition on elastic properties of silicates. In S. Akimoto and M. Manghnani, Eds., High pressure research in geophysics, p. 125–133. Center for Academic Publication, Japan.

Weidner, D.J., Vaughan, M.T., Ko, J., Wang, Y., Liu, X., Yeganeh-haeri, A., Pacalo, R.E., and Zhao, Y. (1992) Characterization of stress, pressure and temperature in SAM85, a DIA type high pressure apparatus. In Y. Syono and M. Manghnani, Eds., High-pressure research: Application to earth and planetary sciences. Geophysics Monograph Series, 67, 13–17.

Zhang, J. and Guyot, F. Thermal equation of state of iron and $Fe_{0.91}Si_{0.09}$. Submitted to Geophysical Research Letters.

Zhang, L., Ahsbahs, H., and Kutoglu, A. (1996) High pressure comparative crystal chemistry and elasticity of garnets from single crystal X-ray diffraction. Abstract supplement No. 1 to Terra Nova, 8, 70.

Zhang, L., Ahsbahs, H., Hafner, S.S., and Kutoglu, A. (1997) Single-crystal compression and crystal structure of clinopyroxene up to 10 GPa. American Mineralogist, 82, 245–258.

Zhang, J., Martinez, I., Guyot, F., Gillet, P., and Saxena, S.K. (1997) X-ray diffraction study of magnesite at high pressure and high temperature. Physics and Chemistry of Minerals, 24, 122–130.

Manuscript received June 19, 1997
Manuscript accepted November 4, 1997